

Solving the Convection-Diffusion Equations via a Multiscale and Discontinuous Galerkin Approach

Enéas Mendes de Jesus[1,2(✉)] and Isaac Pinheiro dos Santos[2,3]

[1] Federal Institute of Espírito Santo (IFES), 660 Augusto Costa de Oliveira St., Piúma, ES 29285-000, Brazil
eneas.jesus@ifes.edu.br

[2] Postgraduate Program in Computer Science (PPGI), Federal University of Espírito Santo (UFES), Av. Fernando Ferrari, 514 - Goiabeiras, Vitória, ES 29075-910, Brazil
eneas.jesus@edu.ufes.br, isaac.santos@ufes.br

[3] Department of Applied Mathematics (DMA), Federal University of Espírito Santo (UFES), BR-101, km 60 - Litorâneo, São Mateus, ES 29932-540, Brazil

Abstract. We present a multiscale and discontinuous Galerkin approach for solving the convection-dominated diffusion problems. The unresolved fine-scales are discretized element-wise using bubble functions. A discontinuous Galerkin discretization is employed in the resolved macro scales. To enhance stability to the numerical formulation, we add a nonlinear artificial diffusion operator inside of the elements, acting on both scales, and an extra stabilization on the interelement edges. Numerical tests demonstrate that the method is stable and accurate in solving transport problems with dominant convection.

Keywords: Convection-Diffusion equations · Convection-dominated · Discontinuous Galerkin · Artificial diffusion · Multiscale discontinuous Galerkin method

1 Introduction

Discontinuous Galerkin (DG) methods have been widely used in solving convection-dominated problems. These methods capture discontinuities well when solving purely hyperbolic problems and have good stability properties when solving convection-diffusion problems with dominant convection. However, DG solutions may suffer nonphysical oscillations in the vicinity of discontinuities and steep gradients. Thus, most DG methods need the addition of some appropriate stabilizing terms to obtain stable numerical solutions [1,3]. Many methods are proposed in the literature to combat the oscillations of DG solutions. Some of them are based on slope limiters [5], artificial diffusion [11,15]; nonlinear multiscale methods [2,3], and post-processing techniques [7,8].

Following the ideas of the NSGS method [12], in [2] a discontinuous and multiscale formulation is presented for solving convection-dominated problems,

© The Author(s), under exclusive license to Springer Nature Switzerland AG 2024
O. Gervasi et al. (Eds.): ICCSA 2024, LNCS 14813, pp. 112–124, 2024.
https://doi.org/10.1007/978-3-031-64605-8_8

where a residual-based nonlinear artificial diffusion operator is added to the fine scales. The amount of artificial diffusion is scaled by the resolved scale solution at the element level. Also, two nested meshes must be built: a mesh representing the macro space and a more refined mesh where the problem is solved. This results in a formulation with a higher computational cost than the classical DG methods. In [3], a modification of this method is presented by introducing the artificial diffusion on both scales. The method proposed in [3] was rewritten in the continuous Galerkin framework using bubble functions to discretize the micro scale [13,14], resulting in a method with good convergence and stability properties. Since this bubble-based method needs only a mesh, it has a computational cost of the same order as the standard continuous Galerkin formulation.

In this work we present a new formulation which rewrites the continuous method [13,14] using broken spaces. The discontinuous framework is applied only on the macro scale, while the fine scales are discretized element-wise using bubble functions. Thus, it requires only a mesh associated with the macro scale to solve the problem. To enhance stability to the numerical formulation, we add a nonlinear artificial diffusion operator inside the elements, acting on both scales, and an extra stabilization on the interelement edges. The new numerical scheme improves stability of the DG methods while being more economical than the discontinuous methods described in [2,3].

The outline of this paper is organized as follows. Section 2 presents the convection-diffusion equation, the concepts and notations used throughout the text, as well as the DG formulation. Section 3 describes the new numerical methodology. Numerical test are discussed in Sect. 4 and Sect. 5 concludes this paper.

2 Discontinuous Galerkin Formulation

Let $\Omega \in \mathbb{R}^2$ be a bounded open domain with Lipschitz boundary Γ. The convection-diffusion-reaction equation is given by

$$\begin{aligned} -\kappa \Delta u + \boldsymbol{\beta} \cdot \nabla u + \sigma u &= f \text{ in } \Omega, \\ u &= g \text{ on } \Gamma, \end{aligned} \tag{1}$$

where $\kappa \in \mathbb{R}$, $\kappa > 0$, is the diffusion coefficient, $\boldsymbol{\beta}$ is the divergence-free velocity field, σ is the reaction coefficient, and f is the source term. We also define the inflow boundary

$$\Gamma_- = \{x \in \Gamma;\ \boldsymbol{\beta}(x) \cdot \mathbf{n}(x) < 0\}, \tag{2}$$

where $\mathbf{n}(x)$ denotes the unit outward normal vector to Γ at $x \in \Gamma$. Moreover, all assumptions for well-posedness, existence and uniqueness of the solution to the problem (1) are considered here, but, for simplicity, are omitted and can be consulted on [6].

Let $\mathcal{T}_h = \{K\}$ be a triangulation of the domain Ω. The area of a triangle $K \in \mathcal{T}_h$ is denoted by $|K|$, and the mesh parameter is $h = \max_{K \in \mathcal{T}_h}\{h_K\}$, where

$h_K = \sqrt{|K|}$. We denote by $\mathcal{E}_h$ the set of all edges in $\mathcal{T}_h$, defined by

$$\mathcal{E}_h = \bigcup_{K \in \mathcal{T}_h} \partial K. \tag{3}$$

The set of internals and boundaries edges are represented by $\mathcal{E}_h^0$ and $\mathcal{E}_h^\Gamma$, respectively. For the inflow edge on the domain boundary and on each element, the notations are $\mathcal{E}_h^{0-}$ and $\mathcal{E}_h^{\Gamma-}$, respectively. Since we use a discontinuous approach, we need to present the definition of typical tools such as averages and jumps on the edges for scalar and vector valued functions. An edge $e \in \mathcal{E}_h^0$ is shared by two elements K_1 and K_2. Let φ be a scalar piecewise smooth function on $\mathcal{T}_h$ with $\varphi^i = \varphi|_{K_i}$. We define the jump and average of φ, respectively, over e as

$$[\![\varphi]\!] = \varphi^1 \mathbf{n}^1 + \varphi^2 \mathbf{n}^2, \ \{\varphi\} = \frac{1}{2}(\varphi^1 + \varphi^2), \tag{4}$$

where $\mathbf{n}^i$ is the outward unit normal vector of K_i on e. To a vector function $\boldsymbol{\tau}$, those definitions are give by

$$[\![\boldsymbol{\tau}]\!] = \boldsymbol{\tau}^1 \cdot \mathbf{n}^1 + \boldsymbol{\tau}^2 \cdot \mathbf{n}^2, \ \{\boldsymbol{\tau}\} = \frac{1}{2}(\boldsymbol{\tau}^1 + \boldsymbol{\tau}^2). \tag{5}$$

For $e \in \mathcal{E}_h^\Gamma$ we set

$$[\![\varphi]\!] = \varphi \mathbf{n}, \ \{\varphi\} = \varphi, \ \{\boldsymbol{\tau}\} = \boldsymbol{\tau}. \tag{6}$$

Following the approach of [9], we shall introduce the variational formulation of (1). The standard notations and definitions of Lebesgue and Sobolev space and their norms will be used. The space of discontinuous piecewise linear functions on Ω is defined as

$$V_h = \{v \in L^2(\Omega) : \ v|_K \in P_1(K), \ \forall K \in \mathcal{T}_h\}, \tag{7}$$

where $P_1(K)$ denotes the space of linear polynomials on element K. The inner products are defined by

$$(u, v)_K = \int_K uv \ d\boldsymbol{x}, \qquad \langle \hat{u}, \hat{v} \rangle_e = \int_e \hat{u}\hat{v} \ ds, \tag{8}$$

where $u, \ v \in L^2(K)$ and $\hat{u}, \ \hat{v} \in L^2(e)$. A discontinuous Galerkin formulation for solving (1) is given as follow: find $u_h \in V_h$ such that

$$B_{DG}(u_h, v_h) = F_{DG}(v_h), \quad \forall v_h \in V_h, \tag{9}$$

where

$$\begin{aligned} B_{DG}(u_h, v_h) = & \sum_{K\in\mathcal{T}_h} (\kappa\nabla u_h, \nabla v_h)_K + \sum_{K\in\mathcal{T}_h} (\boldsymbol{\beta}\cdot\nabla u_h + \sigma u_h, v_h)_K \\ & - \kappa \sum_{e\in\mathcal{E}_h^0} \langle \{\nabla u_h\}, [\![v_h]\!]\rangle_e + \kappa \sum_{e\in\mathcal{E}_h^0} \langle [\![u_h]\!], \{\nabla v_h\}\rangle_e \\ & + \eta \sum_{e\in\mathcal{E}_h^0} \langle [\![u_h]\!], [\![v_h]\!]\rangle_e - \sum_{e\in\mathcal{E}_h^{0-}} \langle \boldsymbol{\beta}\cdot[\![u_h]\!], v_h\rangle_e \\ & - \kappa \sum_{e\in\mathcal{E}_h^\Gamma} \langle \nabla u_h\cdot\mathbf{n}, v_h\rangle_e + \kappa \sum_{e\in\mathcal{E}_h^\Gamma} \langle u_h, \nabla v_h\cdot\mathbf{n}\rangle_e \\ & + \eta \sum_{e\in\mathcal{E}_h^\Gamma} \langle u_h, v_h\rangle_e - \sum_{e\in\mathcal{E}_h^{\Gamma-}} \langle (\boldsymbol{\beta}\cdot\mathbf{n}) u_h, v_h\rangle_e, \end{aligned} \tag{10}$$

$$\begin{aligned} F_{DG}(v_h) = & \sum_{K\in\mathcal{T}_h} (f, v_h)_K + \kappa \sum_{e\in\mathcal{E}_h^\Gamma} \langle g, \nabla v_h\cdot\mathbf{n}\rangle_e \\ & + \eta \sum_{e\in\mathcal{E}_h^\Gamma} \langle g, v_h\rangle_e - \sum_{e\in\mathcal{E}_h^{\Gamma-}} \langle (\boldsymbol{\beta}\cdot\mathbf{n}) g, v_h\rangle_e, \end{aligned} \tag{11}$$

where $\eta = \eta_0\kappa/h$ is a stabilization parameter, and η_0 is a user-chosen parameter. Throughout this work, inspired by [3] and informed by comprehensive testing, we established $\eta_0 = 4$.

3 Multiscale Framework

In this section, we introduce a multiscale approach to reduce spurious oscillations that persist in certain convection-dominated convection-diffusion problems. To achieve this, we consider two scales of discretization. The DG formulation (9) is applied to the macro scale, while bubble functions are employed for the micro scale. Additionally, a nonlinear artificial diffusion operator is added to both discretization scales.

The coarse space, V_h, defined as in (7) is enriched with bubble functions space, defined by

$$V_b = \{w \in H^1(\Omega) : \ w|_K \in H_0^1(K), \ \forall K \in \mathcal{T}_h\}. \tag{12}$$

Here, we use the simple cubic polynomial function $\varphi_b = 27N_1^K N_2^K N_3^K$, where $N_j^K = N_j^K(x, y)$ are the basis function on the V_h space. The enriched space is represented as a direct sum of V_h and V_b, that is,

$$V_E = V_h \oplus V_b. \tag{13}$$

Thus, if $w_E \in V_E$, we can write $w_E = w_h + w_b$ with $w_h \in V_h$ and $w_b \in V_b$.

The proposed method is established from the DG formulation (9) considering the multiscale framework and adding a nonlinear operator defined by

$$D(u_h; u_E, v_E) = \sum_{K \in \mathcal{T}_h} \int_K \xi(u_h) \boldsymbol{\nabla} u_E \cdot \boldsymbol{\nabla} v_E \, d\boldsymbol{x} + \sum_{e \in \mathcal{E}_h} \int_e \eta_1(u_h) [\![u_h]\!] \cdot [\![v_h]\!] ds, \quad (14)$$

where u_E, $v_E \in V_E$.

The first term on the right side of the Eq. (14), defined on the interior of the elements, introduces an artificial diffusion on all scales of discretization, given by

$$\xi(u_h) = \begin{cases} \dfrac{\hbar}{2} \dfrac{|R(u_h)|}{\|\boldsymbol{\nabla} u_h\|}, & \text{if} \quad \|\boldsymbol{\nabla} u_h\| > tol_\xi, \\ 0, & \text{otherwise}, \end{cases} \quad (15)$$

where $\hbar = c_0 \sqrt{|K|}$, $c_0 \in \mathbb{R}$, and tol_ξ is a positive number small enough to avoid division by zero. Throughout this work, we set $tol_\xi = 10^{-5}$. That artificial diffusion is computed dynamically in terms of the residual of the macro scale solution, $R(u_h) = -\kappa \Delta u_h + \boldsymbol{\beta} \cdot \boldsymbol{\nabla} u_h + \sigma u_h - f$, aiming to minimize the kinetic energy related to the unresolved scales [12].

The second term on the right side of the Eq. (14) introduces an extra stabilization term on the edges of the elements belonging to the macro scale mesh since the bubble functions vanish on the edges. A similar term is present in the bilinear form (10), but here, the stabilization parameter, η_1, is given by the average of the artificial diffusion, Eq. (15), calculated in the two elements sharing the edge, that is,

$$\eta_1(u_h) = \eta_0 \frac{\xi^1(u_h) + \xi^2(u_h)}{2h}, \quad (16)$$

where $\xi^i(u_h) = \xi(u_h)|_{K^i}$, $i = 1, 2$ and K^i are the elements sharing the edge.

The variational formulation of the new method is given as follow: find $u_E = u_h + u_b \in V_E$, with $u_h \in V_h$ and $u_b \in V_b$, such that

$$B_{DG}(u_E, v_E) + D(u_h; u_E, v_E) = F_{DG}(v_E), \quad \forall v_E \in V_E, \quad (17)$$

where $v_E = v_h + v_b$, with $v_h \in V_h$, $v_b \in V_b$, $B_{DG}(\cdot, \cdot)$ and $F_{DG}(\cdot)$ are the bilinear and linear operators, respectively, of the discontinuous Galerkin method defined in (10) and (11).

3.1 Nonlinear Process

Since the proposed method insert a nonlinear operator in the discontinuous formulation, an iterative procedure is employed: given u_h^n, we find u_h^{n+1} satisfying

$$B_{DG}(u_E^{n+1}, v_E) + D(u_h^n; u_E^{n+1}, v_E) = F_{DG}(v_E), \quad \forall v_E \in V_E. \quad (18)$$

It is well known that for the continuous approach the discrete nonlinear process has difficulties in converging, a characteristic observed in the majority of nonlinear stabilization schemes [10,14]. To improve the convergence of the iterative process we combine two strategies:

Relaxation scheme as defined in [12]*:*

$$\xi^* \longleftarrow \omega\xi(u_h^n) + (1-\omega)\xi(u_h^{n-1}),$$
$$\xi(u_h^n) \longleftarrow \xi^*,$$

with $\omega = 0.5$;

Freezing of the artificial diffusion presented in [14]*:* if $|R(u^k)|$ is close enough to $|R(u^{k-1})|$ we set $\omega = 0$. In this work we utilize the criterion $|(|R(u^k)| - |R(u^{k-1})|)| < 0.001$ starting from the second iteration.

4 Numerical Experiments

In this section, four standard benchmark problems for convection-diffusion equations are considered to illustrate the behavior of the proposed methodology. Furthermore, the convergence rates of the proposed method in the $L^2(\Omega)$ and $H^1(\Omega)$ norms are evaluated using a problem with a smooth solution. The numerical results are compared with the DG method described in Eq. (9). Despite the numerical formulation considering the reaction term, for our purposes, $\sigma = 0$, and we adopt $c_0 = \sqrt{2}$, so that $\hbar = \sqrt{2|K|}$. In all examples the spatial domain is given by $\Omega = (0,1) \times (0,1)$ and we use a regular triangular mesh with 20 partitions in the x and y directions. All the approximate solutions are represented in a continuous way. To do that, we compute the average of discontinuous solution over each node of the mesh.

4.1 Example 1: Boundary Layers

This problem exhibits parabolic layers at $y = 0$ and $y = 1$ and an exponential layer at $x = 1$. The coefficients of the equation are $\kappa = 10^{-4}$, $\boldsymbol{\beta} = (1,0)^T$, and $f = 1$. Homogeneous Dirichlet boundary conditions are imposed on Γ. In Fig. 1 we represent the approximate solutions obtained by DG method and our method for that problem.

Visually, both the solutions presents overshoots next to the parabolic layer, but these oscillations are more pronounced for DG method. This can be better observed in Fig. 2, where we have represented the profiles of the solutions at $x = 0.8$ and $y = 0.5$. Once the Dirichlet boundary conditions are weakly imposed, oscillations not appear at the exponential layer.

4.2 Example 2: Boundary Layers

The next example consider a problem with non-homogeneous Dirichlet boundary conditions and exact solution. The data of the problem are $\kappa = 10^{-2}$, $\boldsymbol{\beta} = (1,1)^T$ and

$$f(x,y) = 2 + \frac{(1-x)^2 - (1-x) - (1-y) + (1-y)^2}{\kappa(1-e^{-1/\kappa})e^{(1-x)(1-y)/\kappa}} - x - y. \tag{19}$$

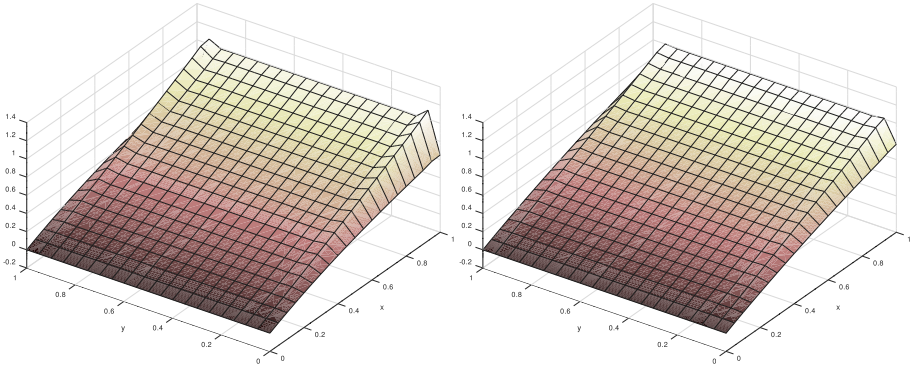
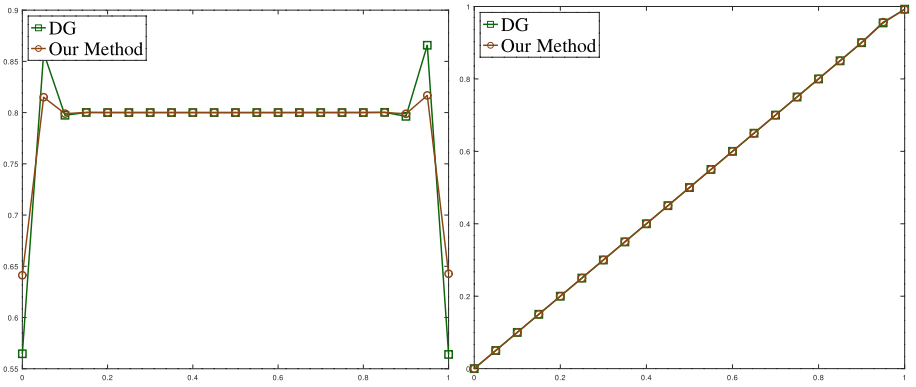


Fig. 1. Example 1. Approximate solutions obtained by DG method (left) and our method (right).



(a) x = 0.8 (b) y = 0.5

Fig. 2. Example 1. Profile of the approximate solutions at $x = 0.8$ and $y = 0.5$ obtained by DG method and our method.

With the following Dirichlet conditions

$$u(x,y) = \begin{cases} 0, & \text{if } x = 1, \text{ or } y = 1; \\ x - \dfrac{(1 - e^{x/\kappa})}{1 - e^{1/\kappa}}, & \text{if } y = 0; \\ y - \dfrac{(1 - e^{y/\kappa})}{1 - e^{1/\kappa}}, & \text{if } x = 0, \end{cases} \tag{20}$$

the analytical solution is given by

$$u(x,y) = x + y(1-x) + \frac{e^{-1/\kappa} - e^{-(1-x)(1-y)/\kappa}}{1 - e^{-1/\kappa}}, (x,y) \in \Omega. \tag{21}$$

If $\kappa \ll 1$ the solution u has a boundary layer along $x = 1$ and $y = 1$. The exact solution and approximations obtained by DG method and our method are depicted in Fig. 3.

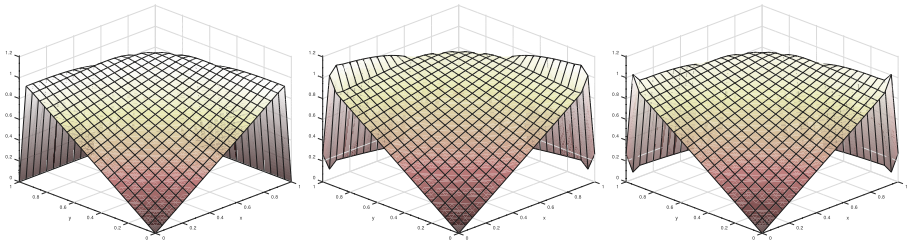


Fig. 3. Example 2. Exact solution (left) and approximate solutions obtained by DG method (center) and our method (right).

Observe that for the chosen data, the DG approximation exhibits oscillations at the boundary layers, whereas the solution obtained by our method is nearly free of oscillation. This can be better observed in Fig. 4, where we have represented the profiles of the solutions along of diagonal, $x = 0.1$ and $y = 0.1$. Notice that an oscillation remains on the inflow boundary next to the points $(0, 1)$ and $(1, 0)$, which can be eliminated using a post-processing, as the exact values of the solution are known on boundary.

4.3 Example 3. Internal Layer

This convection-dominated convective-diffusive problem presents a solution with an internal layer. The velocity field is given by $\boldsymbol{\beta} = (1, 1)^T$, the source term, $f = 0$, and the Dirichlet boundary conditions are defined by

$$u = \begin{cases} 1, & \text{if } x \in [0.3,\ 1],\ y = 0; \\ 0, & \text{otherwise.} \end{cases} \tag{22}$$

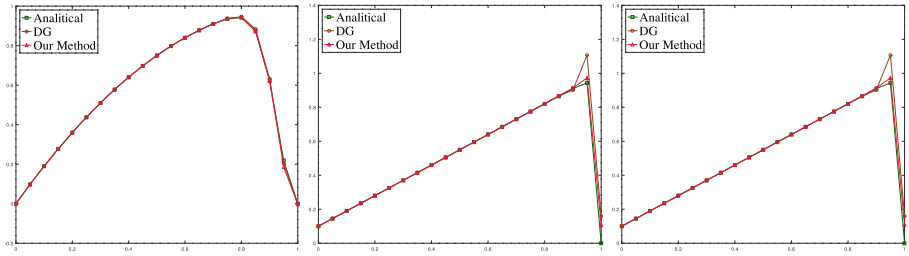


Fig. 4. Example 2. Profile of the exact and approximate solutions at $x = y$, $x = 0.1$, and $y = 0.1$ obtained by DG method and our method.

In the case of a highly convection-dominated problem, DG approximations behave as if the problem were purely hyperbolic [4]. No oscillations occur, since the discontinuity of the inflow boundary propagates to the interior of domain along the direction of convection. In this case, the internal layer is missed in the numerical solution. To represent minimally the internal layer, we adopt $\kappa = 10^{-4}$, considered a moderately convection-dominated problem [8]. In Fig. 5 we represent the approximate solutions where the convection is aligned with the mesh.

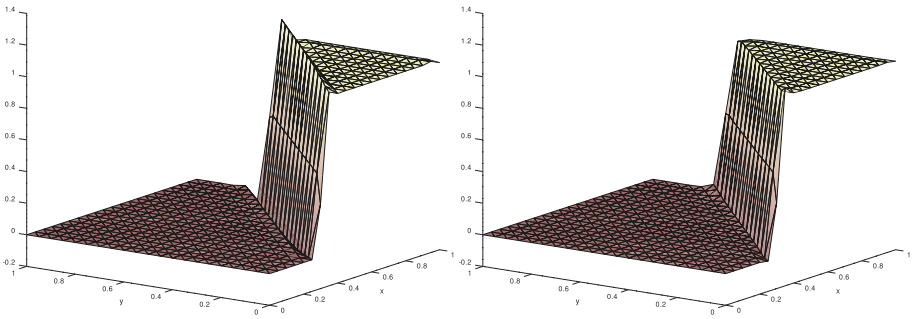


Fig. 5. Example 3. Approximate solutions obtained by DG method (left) and our method (right)

As in the previous examples, the DG approximation exhibits overshoots and undershoots along the internal layer. The current approach reduces the spurious oscillations, leaving only a small oscillation on the inflow boundary next to the discontinuity, which can be addressed with a post-processing technique. This behavior can be observed in Fig. 6.

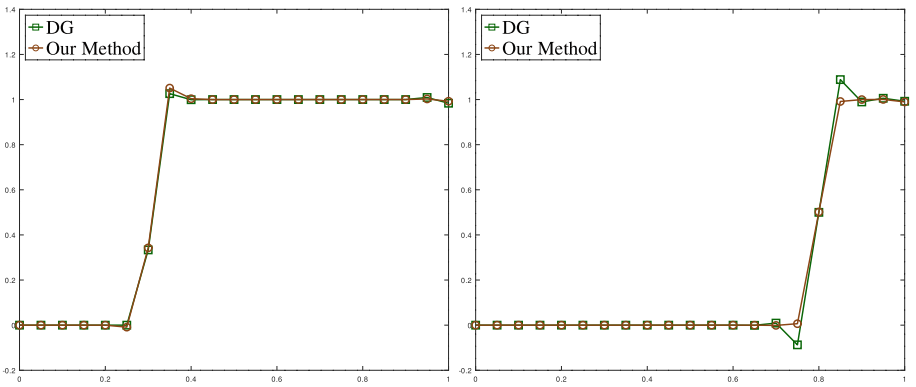


Fig. 6. Example 3. Profile of the approximate solutions at $y = 0$, and $y = 0.5$ obtained by DG method and our method.

4.4 Example 4. Internal Layer

This experiment is basically the same as the previous example, with the only change is the direction of the velocity field $\boldsymbol{\beta}$. While in the previous example, $\boldsymbol{\beta} = (1, 1)^T$, aligned with the mesh, here $\boldsymbol{\beta} = (cos(\pi/6), sin(\pi/6))^T$, not aligned with the mesh. Figures 7 and 8 represent the approximate solutions and some profiles, respectively. Once again, the solution obtained with the new numerical scheme is superior to that obtained by the DG method.

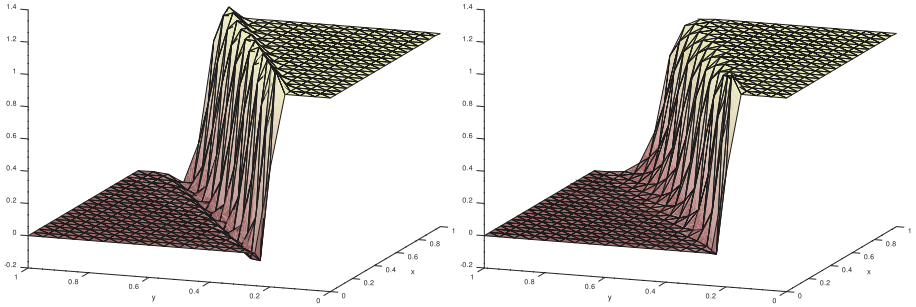


Fig. 7. Example 4. Approximate solutions obtained by DG method (left) and our method (right)

4.5 Convergence Rate

We conclude with a convection-diffusion problem with a smooth solution to evaluate the convergence rates of our method compared with DG method. The convection is given by $\boldsymbol{\beta} = (1, 0)^T$ and f such that $u(x, y) = \sin(\pi x)\sin(\pi y)$ is

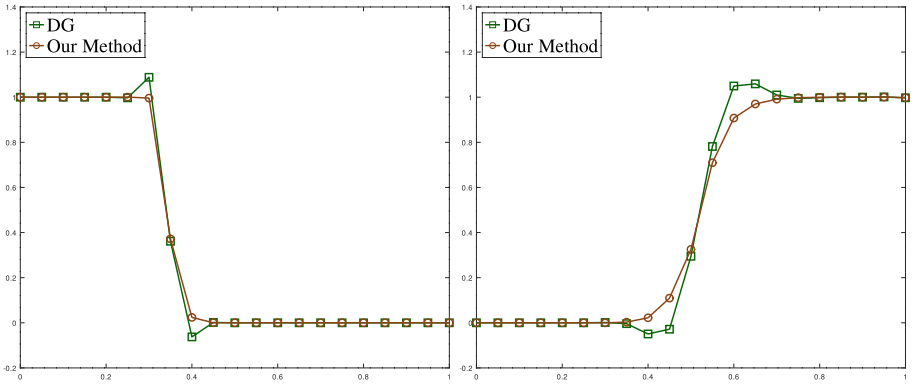


Fig. 8. Example 4. Profile of the approximate solutions at $x = 0.25$, and $y = 0.5$ obtained by DG method and our method.

the exact solution of the problem (1) with $\sigma = 0$ and homogeneous Dirichlet boundary conditions. The approximate solutions are computed for a sequence of five uniform meshes with 128, 242, 450, 800, and 1682 elements. Figure 9 plots the error in $L^2(\Omega)$ associated with the mesh size on a log-log scale. In Fig. 10, under the same conditions, we observe the rates in $H^1(\Omega)$ norm.

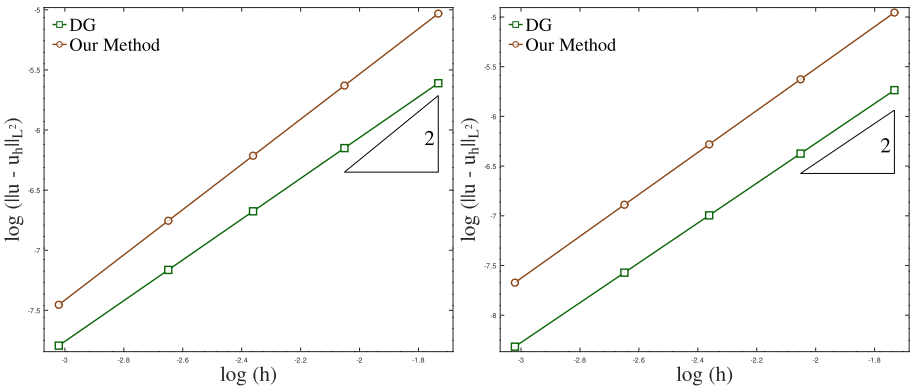


Fig. 9. Convergence rates in the $L^2(\Omega)$-norm considering $\kappa = 10^{-3}$ (left) and $\kappa = 10^{-9}$ (right).

One can note that when the regime is moderately convection-dominated, $\kappa = 10^{-3}$, the DG method exhibits a slight loss of convergence rate. For stronger convection-dominates problem, $\kappa = 10^{-9}$, optimal convergence rates are achieved for both methods. Moreover, the proposed method yields errors in the $L^2(\Omega)$ norm slightly larger than the errors obtained by the DG method.

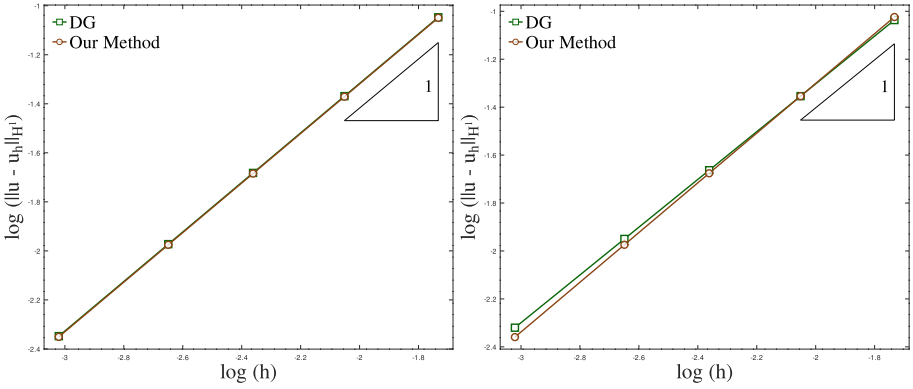


Fig. 10. Convergence rates in the $H^1(\Omega)$-norm considering $\kappa = 10^{-3}$ (left) and $\kappa = 10^{-9}$ (right).

5 Conclusion

This article introduces a multiscale discontinuous Galerkin method for convection-dominated convection-diffusion problems. The methodology involves a discontinuous formulation, which is then enhanced by enriching the resolved space (macro scale) with bubble functions (micro scale). Additionally, to improve the stability of the numerical formulation, we incorporate a nonlinear operator that adds artificial diffusion inside the elements, acting on both scales, along with extra stabilization at the interelement edges. The artificial diffusion is dynamically computed from the residual of the macro scale solution. The edge stabilization utilizes the average of the artificial diffusion of elements sharing each respective edge, making this new stabilization self-adaptive. Numerical experiments demonstrate that the proposed method reduces oscillations in both internal and external layers, with optimal convergence rates observed in the $L^2(\Omega)$ and $H^1(\Omega)$ norms.

Disclosure of Interests. The authors have no competing interests to declare that are relevant to the content of this article.

References

1. Antonietti, P.F., Brezzi, F., Marini, L.D.: Bubble stabilization of discontinuous Galerkin methods. Comput. Methods Appl. Mech. Eng. **198**(21), 1651–1659 (2009)
2. Arruda, N.C.B., Almeida, R.C., do Carmo, E.G.D.: Dynamic diffusion formulation for advection dominated transport problems. Mecanica computacional **XXIX**(20), 2011–2025 (2010)
3. Arruda, N.C., Almeida, R.C., Dutra do Carmo, E.G.: Discontinuous subgrid formulations for transport problems. Comput. Methods Appl. Mech. Eng. **199**(49), 3227–3236 (2010)
4. Ayuso, B., Marini, L.D.: Discontinuous Galerkin methods for advection-diffusion-reaction problems. SIAM J. Numer. Anal. **47**(2), 1391–1420 (2009)
5. Bernardo Cockburn, S.H., Shu, C.W.: The Runge-Kutta local projection discontinuous Galerkin finite element method for conservation laws. IV. The multidimensional case. Math. Comput. **54**(190), 545581 (1990)
6. Di Pietro, D.A., Ern, A.: Mathematical Aspects of Discontinuous Galerkin Methods, vol. 69. Springer, Cham (2011)
7. Frerichs, D., John, V.: On reducing spurious oscillations in discontinuous Galerkin (DG) methods for steady-state convection-diffusion equations. J. Comput. Appl. Math. **393**, 113487 (2021)
8. Frerichs, D., John, V.: On a technique for reducing spurious oscillations in DG solutions of convection-diffusion equations. Appl. Math. Lett. **129**, 107969 (2022)
9. Houston, P., Schwab, C., Süli, E.: Discontinuous HP-finite element methods for advection-diffusion-reaction problems. SIAM J. Numer. Anal. **39**(6), 2133–2163 (2002)
10. John, V., Knobloch, P.: On spurious oscillations at layers diminishing (SOLD) methods for convection-diffusion equations: Part II - Analysis for P1 and Q1 finite elements. Comput. Methods Appl. Mech. Eng. **197**(21–24), 1997–2014 (2008)

11. Persson, P.O., Peraire, J.: Sub-cell shock capturing for discontinuous Galerkin methods. In: 44th AIAA Aerospace Sciences Meeting and Exhibit, p. 112 (2006)
12. Santos, I.P., Almeida, R.C.: A nonlinear subgrid method for advection-diffusion problems. Comput. Methods Appl. Mech. Eng. **196**(45–48), 4771–4778 (2007)
13. Santos, I.P., Malta, S.M., Valli, A.M., Catabriga, L., Almeida, R.C.: Convergence analysis of a new dynamic diffusion method. Comput. Math. Appl. **98**, 1–9 (2021). https://doi.org/10.1016/j.camwa.2021.06.012
14. Valli, A.M., Almeida, R.C., Santos, I.P., Catabriga, L., Malta, S.M., Coutinho, A.L.: A parameter-free dynamic diffusion method for advection-diffusion-reaction problems. Comput. Math. Appl. **75**(1), 307–321 (2018)
15. Yücel, H., Stoll, M., Benner, P.: Discontinuous Galerkin finite element methods with shock-capturing for nonlinear convection dominated models. Comput. Chem. Eng. **58**, 278–287 (2013)